

# CFD Simulation of a Large-diameter Combined Gas Distributor

Xubo Luo<sup>1</sup>, Jinsheng Sun<sup>1</sup>, Jichao Ren<sup>2</sup>, Hong Gao<sup>1</sup>, Linan Li<sup>3</sup> and Chuanxin Pan<sup>4</sup>

<sup>1</sup>School of Chemical Engineering and Technology, Tianjin University, Tianjin, P.R. of China

<sup>2</sup>China Special Equipment Inspection and Research Institute, Beijing, P.R. of China

<sup>3</sup>School of Mechanical Engineering, Tianjin University, Tianjin, P.R. of China

<sup>4</sup>Tianjin University-Runzhida Joint R&D Center, Tianjin, P.R. of China

**Keywords:** Combined Gas Distributor, Computational Fluid Dynamics (CFD), Gas Distribution, Mal-distribution Factor, Pressure Drop.

**Abstract:** In the chemical and process industries, it is a challenge to achieve a uniform initial gas distribution for the packed column with super large diameter and large feed pipeline. This paper suggests a novel combined gas distributor with a large diameter of 6.2m, which integrates a twin-tangential annular flow vapour horn and a shell vane type inlet device (Schoepentoe<sup>TM</sup>, Sulzer Ltd., Switzerland). CFD simulations were carried out to evaluate the performance of the distributor in a column of 6.2m in diameter with a feed pipeline of 3m in diameter. The uniformity of the gas flow on a horizontal plane over the gas distributor was assessed by means of pressure drop and the mal-distribution parameter. Several factors that affect gas distribution, such as the gas inlet velocity, the width of the annular channel, and the split ratio between the radial and annular channels, were analysed comparatively. The gas distribution was found to be more uniform when the annular channel width was 500 mm and the split ratio was 4. Several structural improvements were suggested with their proof simulations showing the superiority of the improved structures over the prototype.

## 1 INTRODUCTION

Packed columns have maintained an important role in process industries, especially in separation processes. These columns are preferred where a high separation performance, a low pressure drop and low liquid loads are required (Olujic et al., 2003b). In a packed column, the feed gas enters the bottom of the column through a gas distributor and flows upward to the top through the packed bed. For most packed distillation columns the initial gas distribution is critical to the overall performance of the whole column. Therefore, many different gas distributors have been developed to achieve uniform initial distribution with no excessive pressure drop.

According to mal-function analysis, gas mal-distribution is one of the main causes of efficiency loss. Although some researches have focused on the gas distribution in columns, these studies neglected the initial gas distribution (Stoter et al., 1993), (Fitz et al., 1999), (Lockett and Billingham, 2003). The initial gas distribution becomes more important

when large diameters, shallow packed beds, and lower pressure drops are simultaneously encountered.

Recently reported experimental studies and CFD analysis of gas phase distribution in packed columns provided evidence of the significant influence that the initial gas distribution has on the separation efficiency (Cai et al., 2003), (Olujic et al., 2003a), (Wehrli et al., 2003).

In the chemical and process industries, there are some cases of shallow packed bed, super large column diameter and large feed inlet diameter, where the uniform initial gas distribution is preferred, with difficulty and challenge. Aiming at these situations, such as a  $\Phi 6200$  column with a  $\Phi 3000$  gas feeding pipeline, this paper suggests a novel combined gas distributor. Shown in Figure 1, it is an assembly of a twin-tangential annular flow vapour horn (TTAF) and a shell vane inlet device (SV), which was initially conceived to improve the gas distribution quality of this special situation. A computational fluid dynamics (CFD) approach was developed to simulate the gas phase distribution in

such combined gas distributor. Detailed systemic data, including gas distribution and pressure drop, was obtained to describe the gas flow that passed through the combined distributor and the upper space. The visible outcomes were then harnessed for structural optimizations.

As to investigate the initial gas distribution and considering the low liquid load of packed column, no counter current liquid was considered in this study. Such method has been also adopted in the published literature (Fan et al., 1997), (Haghshenasfard et al., 2007), (Zhang et al., 2004).

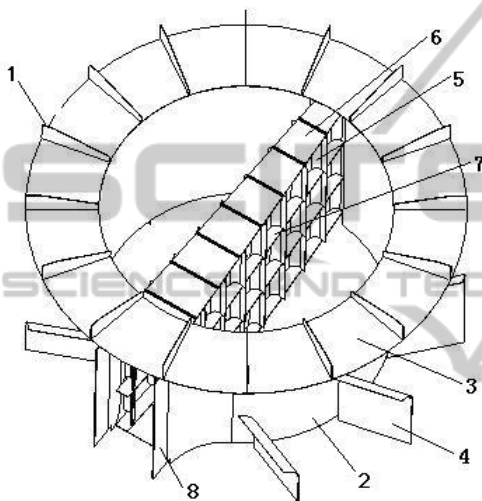


Figure 1: Structure of the combined gas distributor. 1 — web plate; 2 — inside cylinder; 3 — annular channel; 4 — baffle; 5 — vane; 6 — connecting plate; 7 — joint plate; 8 — flapper.

## 2 MATHEMATICAL MODEL AND SOLUTION

### 2.1 Model Equations

A CFD modelling approach is basically solving momentum conservation equations for a computational domain. In this work, under the condition of incompressible gas flow and in the case that user-defined source terms were not considered, the flow governing equations can be simply written as follows (Versteeg and Malalasekera, 1995):

Continuity equation:

$$\nabla(\rho\mathbf{U}) = 0 \quad (1)$$

Momentum equation:

$$\frac{\partial}{\partial t}(\rho\mathbf{U}) + \nabla \cdot (\rho\mathbf{U}\mathbf{U}) = -\nabla P + \nabla \cdot ((\mu + \mu_t)(\nabla\mathbf{U} + (\nabla\mathbf{U})^T)) + \rho\mathbf{g} \quad (2)$$

where  $\rho$  is local fluid density,  $\mathbf{U}$  is the velocity vector,  $P$  is the pressure,  $\mu$  is the viscosity,  $\mu_t$  is the turbulent viscosity and  $\mathbf{g}$  is the gravity acceleration. The fluid was designated to be air with the density  $\rho = 1.225\text{kg/m}^3$  and the viscosity  $\mu = 1.79895 \times 10^{-5}\text{kg/m}\cdot\text{s}$ .

The standard k- $\epsilon$  model has been extensively used to describe the turbulence in gas distributors (Dhotre and Joshi, 2007), (Mohammadkhan and Mostoufi, 2009), (Zhang et al., 2004). Considering the physics encompassed in the flow, the level of accuracy required and the time simulation, the standard k- $\epsilon$  model, which is recognized to be sound and valid in the range of Reynolds numbers for turbulences with intensities from low to moderate, was adopted.

For k

$$\frac{\partial \rho k u_i}{\partial x_i} = \frac{\partial}{\partial x_j} \left[ \left( \mu + \frac{\mu_t}{\sigma_k} \right) \frac{\partial k}{\partial x_j} \right] + G_k - \rho \epsilon \quad (3)$$

For  $\epsilon$

$$\frac{\partial (\rho k u_i)}{\partial x_i} = \frac{\partial}{\partial x_j} \left[ \left( \mu + \frac{\mu_t}{\sigma_\epsilon} \right) \frac{\partial \epsilon}{\partial x_j} \right] + C_{1\epsilon} G_k \frac{\epsilon}{k} - C_{2\epsilon} \rho \frac{\epsilon^2}{k} \quad (4)$$

The generation of turbulence kinetic energy,  $G_k$ , can be computed by:

$$G_k = \mu_t \left( \frac{\partial u_i}{\partial x_j} + \frac{\partial u_j}{\partial x_i} \right) \frac{\partial u_i}{\partial x_j} \quad (5)$$

The constants for the standard k- $\epsilon$  model are assigned as  $C_{1\epsilon} = 1.44$ ,  $C_{2\epsilon} = 1.92$ ,  $C_\mu = 0.09$ ,  $\sigma_k = 1.0$ ,  $\sigma_\epsilon = 1.3$

### 2.2 Computational Domain and Mesh Generation

The CFD simulation was completed for the case of a  $\Phi 6200$  mm diameter column with inlet diameter of  $\Phi 3000$ mm, as illustrated in Figure 2. Considering the space limit in the packed column in industrial application, the gas distribution on the horizontal plane which is 1.2m above the annular plane of the gas distributor was investigated. For the symmetric structure of the gas distributor and the column, only half of the column was simulated.

According to Tu et al. (Tu et al., 2008), the use of hybrid grids can be provided maximum flexibility

in the complex flow region. As a result, for our case, the tetrahedral meshes in the gas distribution region were created by the pre-processor GAMBIT2.4, and the hexagonal grids were adopted in the rest volumes, which are shown in Figure 3. The total number of cells in the computational domain was 427,020.

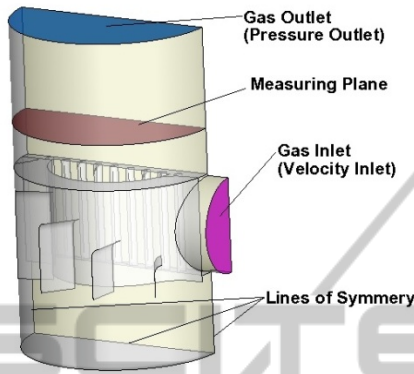


Figure 2: Computational Domain of the CFD simulation.

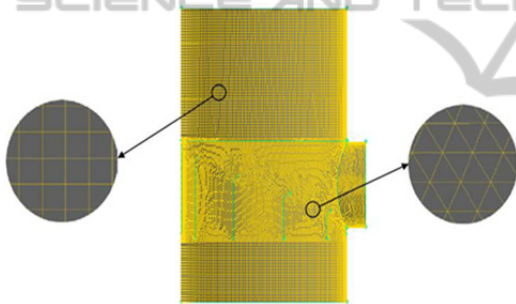


Figure 3: The grid map of the CFD simulation.

### 2.3 Boundary Conditions

To solve the equations of continuity and momentum, appropriate boundary conditions should be specified, as presented in Figure 2. Velocity-Inlet was adopted as the gas inlet boundary, and the velocity, turbulence intensity and hydraulics diameter were set to 30m/s, 5% and 3m, respectively. The gas outlet boundary was specified to be the Pressure-Outlet, and the outlet pressure was set to 101,325Pa. All walls were specified as no-slip wall boundaries. The standard wall function method was used to account for the near regions in the numerical computation of turbulent flow. In addition, at the plane of symmetry, the normal velocity is zero and the gradients of the other variables in the transverse coordinate direction are taken to be zero.

Some assumptions were used to simplify the problem. They are as follows(Haghshenasfard et al., 2007):

- The system is under steady-state conditions.
- The temperature is kept constant.
- The physical properties of the gas flow (air) are constant throughout the column.
- The gas flow at the inlet section of the gas distributors is uniform.
- Phenomena such as flow channelling and back mixing can be neglected in the CFD models.

### 2.4 Numerical Method

The model in our work was solved by virtue of the commercial package FLUENT 6.3.26 (Fluent Inc., USA). In the case of non-high speed and incompressible fluid flow, we chose the segregated solver, which had less memory requirement. The convective terms in the governing equations were modelled with the first-order upwind scheme. The pressure-velocity coupling was obtained by using of the SIMPLE algorithm with default under-relaxations factors. During the simulation progress, the convergence criteria for the residuals, including x-velocity, y-velocity, z-velocity, k, and ε, were set to 0.0001. The calculations of this work were performed on a Dell PC with an Intel Core i7 CPU and 4GB RAM.

## 3 RESULTS AND DISCUSSION

### 3.1 Grid Independence

To confirm that the simulation results are independent of the grid size, the simulations results of pressure drop were compared, which were obtained from cells of 427020, 634809 and 1585497. The pressure drop, ΔP, was defined as the pressure difference between the inlet and the outlet.

$$\Delta P = P_{in} - P_{out} \tag{6}$$

As shown in Table 1, the pressure drop varies slightly when the cell number is more than 427,020. Considering the cost of computation, 427,020 cells are appropriate for this simulation and the results can be considered grid independent.

Table 1: Effect of cell number on pressure drop.

Cell number	427,020	634,809	1,585,497
ΔP (Pa)	1053	1089	1099

### 3.2 Pressure Drop and Mal-distribution

The mal-distribution factor ( $M_f$ ) represents the ability of the distributing device to equalize the gas flow, which is used as a parameter to estimate the uniformity of the gas velocity parameter (Petrova et al., 2003). It is evaluated at a certain horizontal plane in the column at the height of 1.2m above the annular channel, with the following equation:

$$M_f = \sqrt{\frac{1}{n} \sum_{i=1}^n \left( \frac{U_i - U_0}{U_0} \right)^2} \quad (7)$$

where  $n$  is the total number of the sample points,  $U_i$  is the local gas velocity at every point, and  $U_0$  is the superficial gas velocity, which is defined as the average gas velocity of the investigated plane. The sample points are shown in Figure 4. As the mal-distribution factor decreases, it leads to a uniform distribution of gas flow in the columns (Olujic et al., 2003a).

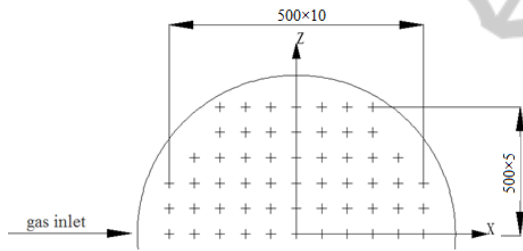


Figure 4: Distribution of the sample points.

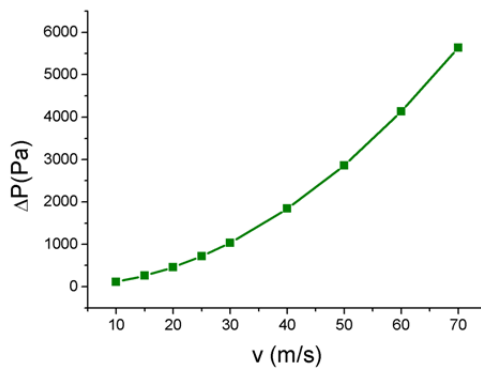


Figure 5: The simulation result of pressure drop at different inlet velocities.

The pressure drop and mal-distribution at different inlet velocities are shown in Figure 5 and Figure 6, respectively. The pressure drop becomes larger as the inlet velocity increases, whereas the mal-

distribution remains constant as the inlet velocity varies from 10m/s to 70m/s. This regularity indicates that the performance of the combined gas distributor lies in the structure itself rather than in the inlet velocity in this range.

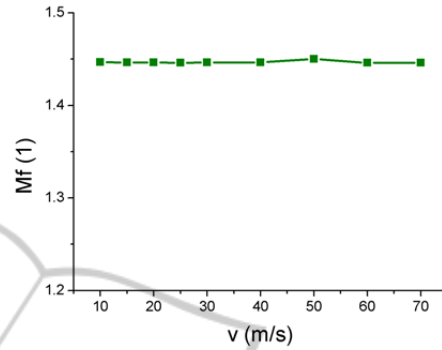


Figure 6: The simulation result of mal-distribution factor at different inlet velocities.

### 3.3 Effect of Width of the Annular Channel

The width of the annular channel,  $w$ , observably influences the performance of the combined gas distributor. Figure 7 and Figure 8 show the pressure drops and mal-distribution factors at different widths of the annular channel, respectively. Both pressure drop and mal-distribution, evidently, are small when the width falls from 400 mm to 800 mm. Specifically, when the width is less than 400 mm, the outside flow path is too narrow for the gas flow, leading to a large pressure loss in the front of the combined gas distributor, consequently worsening the distribution. In contrast, when the annular tunnel is wider than 800 mm, the sectional area of the flow path is squeezed to increase the gas flow resistance greatly, worsening the gas distribution as well. By comparison, 500 mm is considered the optimal width of the annular channel.

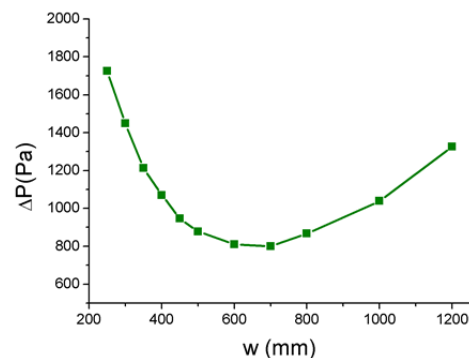


Figure 7: Effect of the width of the annular channel on pressure drop.

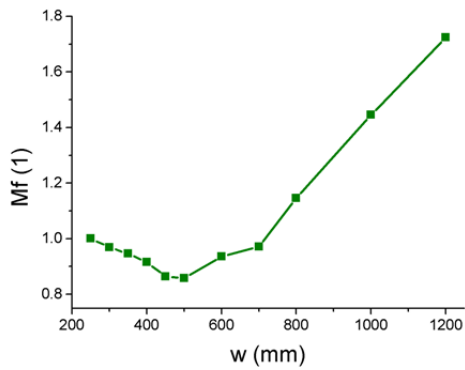


Figure 8: Effect of the width of the annular channel on pressure drop and mal-distribution factor.

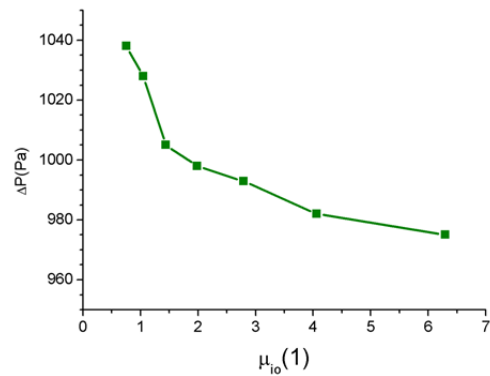


Figure 9: Effect of split ratio on pressure drop.

### 3.4 Effect of Split Ratio

The two parts of the combined gas distributor, TTAF and SV, have advantages and disadvantages. TTAF is not appropriate for large-diameter inlets because of the abrupt change in the flow cross-sectional area; SV is also not appropriate because of its narrow entrance. Thus, the split ratio of the inlet gas flow,  $\mu_{10}$ , is an important factor that influences the performance of the distributor.

The split ratio is controlled by the exact position of the flappers, and the corresponding relation of the two factors is shown in Table 2.

The effect of the split ratio on pressure drop is shown in Figure 9 and the effect on mal-distribution factor is in Figure 10. An unremarkable effect of split ratio is gained by analysing. However, the increasing split ratio caused a decreased pressure drop and the same mal-distribution factor with respect to widening the annular channel. When the split ratio was 4, the performance of the gas distributor was optimal.

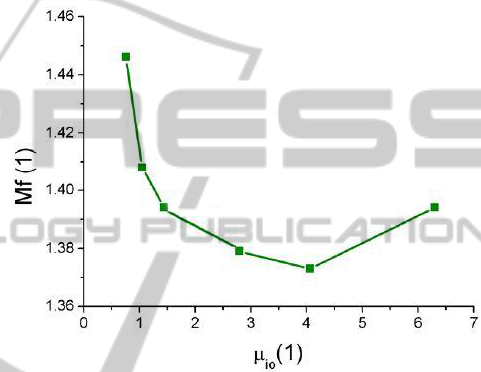


Figure 10: Effect of split ratio on mal-distribution factors.

Table 2: split ratios at different inlet flapper positions.

Distance between the two flappers (mm)	Split ratio
1000	0.755
1200	1.047
1400	1.438
1600	1.985
1800	2.790
2000	4.061
2200	6.295

## 4 STRUCTURAL IMPROVEMENTS

Figure 11 shows the velocity vector in the column. The low speed regions and vortices upon the annular channel, as well as the high speed zone of the inside path above the distributor, are shown. The abrupt change in the sectional area on the top of the distributor is the primary factor that influences the performance of the distributor.

According to the analysis above, six kinds of structural improvements were proposed, as shown in Figure 12.

All types of structural improvements, determined by CFD analysis, improved the performance of the distributor. The optimization comparisons of the pressure drop and the mal-distribution factors for every type of improvement are listed in Table 3. It can be recognized that the effects of the six variations are all positive. The structure patterns of d and f result in the best mal-distribution factors, while the f and g patterns have the greatest benefit on the pressure drop. In summary, the structure f can be

considered as the best structure pattern among the six variations.

Table 3: Pressure drop and Mal-distribution of different structure patterns.

Structure	$\Delta P(\text{Pa})$	Fall(%)	$M_f(-)$	Fall(%)
Prototype a	1053	-	1.446	-
Structure b	977	7.2	1.322	8.7
Structure c	834	20.7	0.946	34.6
Structure d	842	20.0	0.831	42.5
Structure e	825	21.6	0.899	37.8
Structure f	782	25.7	0.833	42.6
Structure g	771	26.8	0.863	40.3

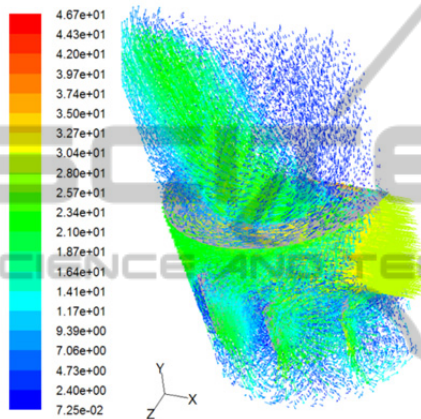


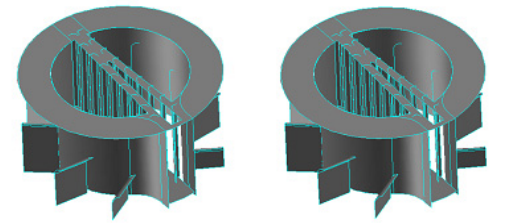
Figure 11: Velocity vector in the column (the column diameter is  $\Phi 6200$  mm and the inlet diameter is  $\Phi 3000$  mm).

## 5 CONCLUSIONS

This work presents a three-dimensional CFD model based on the novel combined gas distributor of a large diameter, which integrates of a Twin-Tangential Annular Deflector Gas Distributor and a Two-Line Vane Gas Distributor. The gas distributor was investigated numerically, where the pressure drop and mal-distribution factor were adopted to assess the uniformity of the gas distribution in the columns. According to the CFD analysis, the mal-distribution factor is hardly affected by the inlet velocities. In addition, the gas distribution was found to be the most uniform when the width of annular channel was 500 mm and the split ratio was 4 for a  $\Phi 6200$  mm column.

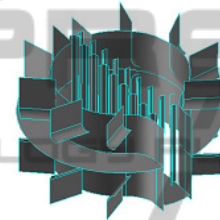
According to the CFD results, six types of structural improvements were suggested, which were able to improve the uniformity of gas flow in the column, and the type which remove the annular channel from the prototype has been confirmed as the best type among the six. These improvements

provide guidance for the further optimization of the design of gas distributors.

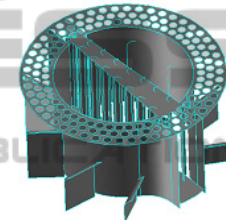


(a) prototype

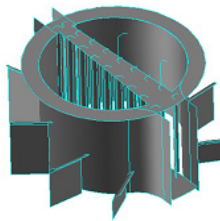
(b) isosceles triangle hole on cover board (the length of base side is 450 mm, and the height of triangle is 4000 mm)



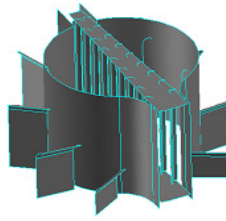
(c) moving the annular channel down (the size of downward shift is 1500 mm)



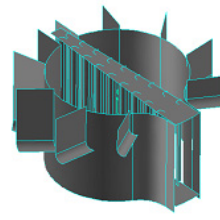
(d) equispaced holes in the annular channel (the hole diameter is 240 mm)



(e) annular hole in the annular channel (the width of annular hole is 400 mm)



(f) no annular channel



(g) reversed baffles and no annular channel

Figure 12: Structural improvements.

## SYMBOLS USED

$C_{1\varepsilon}$	[-]	model constant
$C_{2\varepsilon}$	[-]	model constant
$C_{\mu}$	[-]	model constant
$g$	$[\text{m}\cdot\text{s}^{-2}]$	acceleration of gravity
$G_k$	$[\text{kg}\cdot\text{m}^{-1}\cdot\text{s}^{-1}]$	production of turbulent kinetic energy
$k$	$[\text{m}^2\cdot\text{s}^{-2}]$	turbulent kinetic energy
$M_f$	[-]	mal-distribution factor
$n$	[-]	number of sample points
$P$	[Pa]	pressure
$\Delta P$	[Pa]	pressure drop
$t$	[s]	time
$U$	$[\text{m}\cdot\text{s}^{-1}]$	interstitial velocity
$U_i$	$[\text{m}\cdot\text{s}^{-1}]$	local velocity
$U_0$	$[\text{m}\cdot\text{s}^{-1}]$	superficial velocity
$w$	[mm]	width of the annular channel
Greek symbols		
$\varepsilon$	$[\text{m}^2\cdot\text{s}^{-3}]$	turbulent energy dissipation
$\rho$	$[\text{kg}\cdot\text{m}^{-3}]$	density
$\mu$	$[\text{kg}\cdot\text{m}^{-1}\cdot\text{s}^{-1}]$	viscosity
$\mu_t$	$[\text{kg}\cdot\text{m}^{-1}\cdot\text{s}^{-1}]$	turbulent viscosity
$\mu_{io}$	[-]	split ratio
$\sigma_k$	[-]	model constant
$\sigma_t$	[-]	model constant
$\Phi$	[mm]	diameter
Subscripts		
$i, j$		coordinate index
in		inlet
out		outlet

## REFERENCES

- Cai, T. J., Chen, G. X., Fitz, C. W. & Kunesh, J. G. 2003. Effect Of Bed Length And Vapour Maldistribution On Structured Packing Performance. *Chemical Engineering Research & Design*, 81, 85-93.
- Dhotre, M. T. & Joshi, J. B. 2007. Design Of A Gas Distributor: Three-Dimensional Cfd Simulation Of A Coupled System Consisting Of A Gas Chamber And A Bubble Column. *Chemical Engineering Journal*, 125, 149-163.
- Fan, L., Chen, G., Constanzo, S. & Lee, A. 1997. Hydraulic Performance Of Gas Feed Distribution Devices. *Icheme Symp Ser.*
- Fitz, C. W., King, D. W. & Kunesh, J. G. 1999. Controlled Liquid Maldistribution Studies On Structured Packing. *Chemical Engineering Research & Design*, 77, 482-486.
- Haghshenasfard, M., Zivdar, M., Rahimi, R. & Esfahany, M. N. 2007. Cfd Simulation Of Gas Distribution Performance Of Gas Inlet Systems In Packed Columns. *Chemical Engineering & Technology*, 30, 1176-1180.
- Lockett, M. J. & Billingham, J. F. 2003. The Effect Of Maldistribution On Separation In Packed Distillation Columns. *Chemical Engineering Research & Design*, 81, 131-135.
- Mohammadkhan, A. & Mostoufi, N. 2009. Effect Of Geometry Of The Plenum Chamber On Gas Distribution In A Fluidized Bed. *Industrial & Engineering Chemistry Research*, 48, 7624-7630.
- Olujic, Z., Ali, A. M. & Jansens, P. J. 2003a. Effect Of The Initial Gas Maldistribution On The Pressure Drop Of Structured Packings. *Chemical Engineering And Processing*, 43, 465-476.
- Olujic, Z., Kaibel, B., Jansen, H., Rietfort, T., Zich, E. & Frey, G. 2003b. Distillation Column Internals/Configurations For Process Intensification. *Chemical And Biochemical Engineering Quarterly*, 17, 301-309.
- Petrova, T., Semkov, K. & Dodev, C. 2003. Mathematical Modeling Of Gas Distribution In Packed Columns. *Chemical Engineering And Processing*, 42, 931-937.
- Stoter, F., Olujic, Z. & De Graauw, J. 1993. Modelling And Measurement Of Gas Flow Distribution In Corrugated Sheet Structured Packings. *The Chemical Engineering Journal And The Biochemical Engineering Journal*.
- Tu, J., Yeoh, G. H. & Liu, C. 2008. *Computational Fluid Dynamics -A Practical Approach*, Amsterdam, Elsevier Inc.
- Versteeg, H. K. & Malalasekera, W. 1995. *An Introduction To Computational Fluid Dynamics: The Finite Volume Method*, New York, Wiley.
- Wehrli, M., Hirschberg, S. & Schweizer, R. 2003. Influence Of Vapour Feed Design On The Flow Distribution Below Packings. *Chemical Engineering Research & Design*, 81, 116-121.
- Zhang, L. H., Zhou, H. Y., Li, X. G. & Du, Y. P. 2004. Cfd Analysis Of Gas Distributor In Packed Column - Prediction Of Gas Flow And Effect Of Tower Internals Geometry Structure. *Transactions Of Tianjin University*, 10, 270-274.